Examination of organic coatings on metallic substrates by scanning electrochemical microscopy in feedback mode: revealing the early stages of coating breakdown in corrosive environments

Ricardo M. Souto, Yaiza González-García, Javier Izquierdo, Sergio González

Department of Physical Chemistry, University of La Laguna, E-38207 La Laguna, Tenerife, Canary Islands, Spain

Abstract

Scanning electrochemical microscopy in feedback mode was used to monitor changes in the surface state of a polymeric film applied on a metallic substrate when exposed to an aqueous electrolytic environment. The protected metal consisted of a carbon steel substrate coated with a polyurethane-based polymeric film. SECM measurements performed in the presence and absence of chloride anions permitted a specific effect caused by Cl- anions at early exposures to be detected. Significant surface roughening is observed for immersion times shorter than one day when the electrolyte contains chloride ions. Additionally, the growth of an individual blister could also be investigated.

Keywords: Scanning electrochemical microscopy; organic coatings degradation; blistering; polyurethane; mild steel.

1. Introduction

One of the most convenient, and certainly the oldest method of protecting a substrate from the detrimental effects of the environment, is to coat it with some barrier to isolate it from its surroundings. Organic coatings are applied to produce a relatively continuous, inert and adherent film between the surface of the metal and the environment, which would hinder the transport of aggressive species from the environment towards the metal/polymer interface [1,2]. Though water and oxygen are necessary agents for the initiation of the corrosion reaction and they are also known to exhibit high permeabilities through a variety of resin binders, the question remains open as to whether the limiting factor in the protective mechanisms of barrier coatings is their resistance to the flow of ionic current and the formation of an extended diffuse layer [3]. That is, the corrosion protection characteristics of the coatings would depend on the specific electrochemical properties of the metal/polymer interface rather than on the transport of water and oxygen. Indeed, the composition, polymer network density, general polymer bulk structure and thickness of the coating are of ultimate importance [4].

Since ion permeation is regarded to be significantly slower than those of oxygen and water, corrosion in coated metals is believed to occur after the formation of conductive pathways through the polymeric matrix where the aggressive ions can diffuse from the electrolytic solution towards the unprotected metal. Thus, corrosion can be regarded to initiate at “weak points” or sites of mechanical damage in the coatings, either from pores resulting from the physical drying or curing stages of the resin, or from defects such as scratches, pinholes or cut edges produced during the forming and handling steps of the coated material for service. Transport phenomena in organic coatings and the corrosion behaviour of coated metals are thoroughly investigated using electrochemical impedance spectroscopy (EIS) [2,5], including novel methods such as dynamic electrochemical impedance spectroscopy (DEIS) which allows the obtention of instantaneous impedance spectra [6], thus enabling tracing fast processes such as those related to transport within organic coatings. Furthermore, the recent introduction in the corrosion laboratory of spatially-resolved microelectrochemical techniques such as the scanning Kelvin probe (SKP) [7-14], scanning vibrating electrode technique (SVET) [15-25], localized electrochemical impedance (LEIS) [26-28] and scanning electrochemical microscopy (SECM) [29-32], is providing new mechanistic insights into the highly localized corrosion processes occurring at coated metals. Namely, SKP has been

successfully employed in the monitoring of the degradation processes at the buried metal/polymer interface related to delamination fronts [8-14] and to filiform corrosion [7], whereas SVET, LEIS and SECM effectively monitor electrochemical activity from defects in coatings such as cut edges [15-17,20,23,24], pinholes [18,22,25,27,30] and scratches [19,21,26,28,29,32].

But even apparently uniform coatings are also known to undergo corrosion. We have recently reported a specific effect of chloride ions leading to non-uniform damage of an intact polyester coating applied on galvanized steel as monitored by scanning electrochemical microscopy [33]. Blister formation at early exposures was observed to occur only in chloride-containing solutions above a given threshold concentration for the anion [34], and to happen for polyester coated samples on galvanized steel for various compositions of the zinc-based metallic layer [35]. These observations showed that chloride caused damage to the organic coating almost immediately after immersion, but this did not occur when the polyester films were immersed in sulphate solution. The eventual uptake of salt from the solution by the coating accompanying the initial ingress of water was proposed to be considered in order to justify the swelling of coil-coated cladding observed at a very early stage after immersion in chloride solution [33]. Questions remain concerning whether specific anion effects can also be observed from other polymeric structures and binder compositions, as well as for other underlying metallic substrates, and concerning how the aggressive ions from the electrolyte penetrate through the coating.

In the present work, the role of chloride ions towards the early swelling of carbon steel coated by a polyurethane film was studied by means of scanning electrochemical microscopy in feedback mode. Scanning electrochemical microscopy operating in the feedback mode is specially suited for such investigation [36], because the near-field behaviour of the electrochemical probe is affected by the conductivity characteristics of the substrate. In the case of an insulating sample, the current sensed at the tip for the electrochemical conversion of a suitable redox mediator decreases as the tip approaches the substrate (negative feedback). Constant-height rastering of the sample's surface with the microelectrode tip delivers topographical images in the case of chemically-homogeneous substrates. And the variations in the current measured at the tip directly correlate to tip-substrate distances by using the corresponding approach curves [37]. In order to discard any interference arising from the addition to the test environment of a

freely diffusing redox mediator for imaging purposes at the ultramicroelectrode tip, additional experiments were performed in which the irreversible reduction of dissolved oxygen at the SECM tip was employed for monitoring [38,39]. In this way, the applicability of the scanning electrochemical microscope to both detect the early swelling and the formation of blisters on coated metals was confirmed, and the potentialities of the technique towards the monitoring of the growth of single blisters was demonstrated.

2. Experimental

Materials. Mild steel samples (1 cm x 2 cm) were cut from pannels that had been degreased by dipping in acetone, and coated with a polyurethane resin (*Sigmadur Gloss* from Sigma Coatings, Amsterdam, The Netherlands), applied by draw-down bar [40]. The coupons were allowed to cure for a week at room temperature and humidity prior to testing. The dry film thickness of the coating measured using Mega-Check FN coating thickness-meter (List-Magnetik GmbH, Germany) was chosen in the range 60 μm. The samples were then exposed to aerated aqueous solution at room temperature (~ 20 ºC), and examined using SECM at regular intervals. Test electrolytes were either 0.1 M KCl or K_2SO_4 solutions prepared using analytical grade chemicals and 18 MΩ cm^{-1} water.

Scanning electrochemical microscopy. The SECM instrument used in these experiments was a Sensolytics scanning electrochemical microscope (Sensolytics, Bochum, Germany), which is controlled by a control unit and software. The system was placed inside an active isolation workstation, which effectively isolated the system from electrical and acoustic noise as well as from mechanical vibrations. Control of the microelectrode was performed using a step motor driven *x*-, *y*-, *z*-stage (Owis GmbH, Staufen, Germany) capable of reproducible three-dimensional motion. The electrochemical interface was a bipotentiostat (Palmsens, Utrecht, The Netherlands), though the system was operated in a three-electrode configuration since the coated sample was left unbiased during experiments at its corresponding open-circuit potential.

Experimental procedure. The sample was located at the bottom of a small flat cell, thus exposing the coated side upwards to the test solution. Platinum microelectrodes (10 μm diameter) were employed. They were prepared from 10 μm platinum wires sealed in glass. A video microscope was used to aid microelectrode positioning. An

Ag/AgCl/saturated KCl reference electrode, and a stainless steel wire used as counter electrode were also introduced in the electrochemical microcell. All tip potentials cited in this paper are referred to the Ag/AgCl/saturated KCl reference electrode.

Ferrocene-methanol of concentration 0.5 mM was added to the test electrolyte solutions to act as electrochemical mediator at the tip. To enable the oxidation of the ferrocene-methanol the tip was kept at a constant potential of +0.5 V (Ag/AgCl) [35]. In order to discard any specific effects due to this compound on the behaviour of the investigated system, some experiments were also conducted in the test solution without the addition of ferrocene-methanol. In this case, dissolved oxygen occurring in the naturally aerated cell was employed as electrochemical mediator by setting the tip potential to -0.60 V (Ag/AgCl) [35,39]. The operating distance of the microelectrode tip over the coated surface was set at 15 μm by measuring the corresponding approach curves as previously described [35]. Images were acquired by moving the microelectrode in a raster-type motion. Line scans were acquired in the same scan direction using a step/acquire scheme where the step size was 10 μm. The scan rate was 30 μm s^{-1}. The reproducibility of the results described below was established by imaging a minimum of 5 specimens in each case.

3. Results

The experiments consisted in the detection of the changes occurring in the topography of the coated metal during its exposure to the aqueous solution. Lateral scans across a sample surface result in 3D maps of surface topography. Since the changes in the current values measured at the microelectrode are related to the distance between the tip and the surface directly below it, the topographic features of the coating film were discovered as the microelectrode passed above them. The images are most times plotted with the current axis inverted in order to match the topography of the surface. That is, smaller absolute currents were measured at those locations on the sample which were effectively closer to the SECM-tip rastering over the sample in a constant height mode.

The peculiar behaviour of chloride ions when present in the aqueous solution in contact with a coated sample is clearly deduced from the observation of figure 1. This figure displays the changes occurring in the surface of the samples during their immersion in the test environment for one day. The same area has been scanned for each sample during the experiment. Measurements were performed in both KCl and K_2SO_4 solutions of

0.1 M concentration which are depicted here for the sake of comparison. Though the surface of both samples appeared flat and featureless immediately after immersion in the electrolytes, the topographies were observed to be dramatically different for the specimens after their immersion for 24 hours in each environment. The surface did neither present any kind of damage nor reveal local swelling during its exposure to 0.1 M potassium sulphate solution (cf. figure 1B). But, bulges were found in all directions on the surface of the polyurethane-coated sample after 24 hours exposure to the chloride-containing solution.

It is important to note that the electrolyte could not penetrate along the coating-metal interface starting from the cutting edges of the sample, for the electrochemical flat cell was built such that the area under investigation was isolated by using an o-ring. That is, the edges were not exposed to the electrolyte. This leaves penetration from the electrolyte to the metal-polymer interface only to occur across the coating. Furthermore, before considering transport to have occurred through the polymer matrix, the possible existence of ionic pathways through pores or defects in the coating had to be discarded as well. It is known that coating degradation processes can be favoured by the existence of undesirable failures in the coating, which may become filled with the electrolyte leading to the establishment of an ionic pathway for the transport of the species present in the test environment, including the redox mediator, to reach the metal surface. Thus, it is necessary to secure that all the studied samples were free from such defects, at least of those of large size (greater than 1 μm). Indeed, if the detected blisters had originated from defects in the coating, it should be expected that the defects would grow in size whereas the blisters developed. And even in the case of the smaller defects, though they could not be topographically resolved in the maps obtained with a 10 μm diameter tip, they would have been anyway discovered in our experiments as sudden bursts of faradaic current when the tip passed above the active pore. That is, the onset of a highly localized positive feedback due to the regeneration of the redox mediator at the metal surface should be detected at the tip. Indeed this is the case for the maps shown in figure 2, where such micropores could be detected in the scanned sample at various locations on the sample since early exposure to the test electrolyte. Current bursts continue to be observed during the remaining of the experiment, as shown in figure 2B after 5 hour exposure. Though the current in each peak is resolved to only one point in one line scan, the current measured at that location is significantly higher than the current from the surrounding surface, a

definite evidence of the occurrence of positive feedback at this defective sample. Conversely, current bursts were not detected in any of the maps displayed in figure 1, and can be regarded to correspond to surfaces relatively free of flaws of continuity.

The reported specific effect of chloride ions towards the initiation of blistering under polyurethane-coated carbon steel samples was also observed when dissolved oxygen was employed as electrochemical mediator instead [18], that is, when the test electrolyte was free from ferrocene-methanol. From the inspection of the images depicted in figure 3 it can be concluded that heterogeneous roughening of the coated surface consistent with the development of bulges occurs in 0.1 M KCl solution. Thus, these maps can be considered as a probe that ferrocene-methanol did not significantly perturb the system as it was expected since the redox mediator did not get in contact with the underlying metal in the case of an intact coating. Yet, from the comparison of figures 1 and 3 it is concluded that better resolution of the surface topography was found when ferrocene-methanol was employed as redox mediator.

4. Discussion

Significant surface roughening of polyurethane coated steel which originates from heterogeneous swelling of the polymer induced by chloride ions has been demonstrated by SECM operating in the feedback mode. Though the method depends on redox reactions to proceed at the tip for topographical features to be imaged as result of the hindrance to diffusion imposed by an insulating surface located in close proximity to the rastering microelectrode, the measurements could also be performed without the addition of a freely diffusing mediator to the electrolyte. In this way, heterogeneous roughening of the coating surface during exposure to the chloride-containing environment was effectively imaged when the potential at the tip led to the reduction of dissolved oxygen. This observation is a strong evidence that the observations made when ferrocene-methanol was added to the test electrolyte both in this work and in previous contributions can be sustained in the case of an intact coating as regards to the transport of species from the solution phase into the polymer matrix, including the specific effect of chloride ions towards coating damage.

We attribute the observed features to the nucleation and growth of blisters at the metal/coating interface. Additionally, the advancement towards the tip of individual features formed on the polyurethane coating can also be investigated. In this case, a smaller area should be continuously scanned to produce a sequence of images from which

the nucleation and subsequent evolution of a single feature formed on the polyurethane coating that effectively advances towards the tip could be investigated as a function of elapsed time. For instance, during one single experiment lasting 5 hours, an area of 200 μm x 200 μm could be scanned every 10 minutes. In this way, 30 maps were obtained, a small selection of which are displayed in Figure 4. For the sake of comparison, the corresponding map for the same surface region after 22 hours exposure is also included in Figure 4D. At this stage, two trends could observed from these images, namely, (1) the current range covered in each map corresponds to smaller currents as time elapses, which is consistent with a decrease in the distance between the surface and the tip. This means that the whole surface is effectively approaching the tip, which is always scanned at a constant height, as the result of water uptake from the electrolyte. Nevertheless, between the first and the second maps shown, the trend is exactly the opposite, thus indicating that some lixivation from the polymer may have occurred during the first hour of exposure with the net result of polymer shrinkage. Thus, during the early exposure of the sample, water uptake of water was counteracted by lixiviation from of the polymer with the result that the surface of the coating effectively retracted in average from the tip. And (2), the width of the current range covered in the first map is significantly smaller than in the others, an indication that the difference between summits and valleys within the scanned region of the coated surface effectively increases in time which was expected to happen as the surface becomes rougher due to chloride transport through the coating.

The distance between the summit of a blister and the microelectrode could be quantitatively determined from the current measured at the tip when placed over it by using the approach curve measured over the polyurethane-coated sample, which is depicted in figure 5. The progression towards the microelectrode of the blister detected in figure 4 during the exposure of the coated sample to the chloride-containing solution, was thus followed from the position of the summit point in each map. Figure 6 exhibits the evolution of the distance between the tip and the blister during during 5 hours. Within the first hour of immersion, the coating retracted locally from the microelectrode for a maximum distance of 2.7 μm (Zone I). The coating actually shrinked during the process, an indication that some components lixiviated from the polymer matrix simultaneously to water uptake from the electrolytic solution. At longer exposures, roughening of the surface occurs with the formation of bulges, and a steady trend growth of the blister is maintained for the rest of the experiment (Zone II). That is, the coating advanced locally towards the

solution phase for about 13 μm during the next 4 hours of exposure. This feature was induced by the presence of chloride ions in the solution phase.

Since the formation of such blisters was observed to occur on polyester-coated galvanized steel before [37-39], the reported effect can be considered to be of a more general occurrence and it may be observed to occur for other resin binders and metal substrates as it also happens on polyurethane-coated carbon steel. Therefore, the early formation of blisters must originate from the action of a species present in the aggressive environment, and it occurs even from the first moments of their exposure to a chloride-containing solution. Indeed, the reasoning behind the experiments described in this work was to demonstrate that the early swelling and blistering of coated metals in chloride-containing aqueous solutions is exclusively caused by the nature of the aggressive solution, independently of the chemical nature of the polymer matrix.

4. Conclusions

A novel experimental design for the *in situ* examination of organic coatings on metallic substrates has been described, capable of revealing the early stages of coating breakdown in corrosive environments and the specific effect related to chloride ions. Though the method depends on redox reactions to happen at the SECM tip for imaging purposes, the reported effects were also observed without the addition of a freely diffusing mediator by using dissolved oxygen instead, and the eventuality of interferences due to operation with ferrocene-methanol could be discarded at this stage.

The earlier stages of blister formation in the case the coating covers the surface without flaws of continuity have been detected by SECM. The observed features do not merge and get located in fixed positions at these early stages of coating degradation. Though blister nucleation is an early stage of coating breakdown, from our current measurements we cannot establish whether every nucleated blister may lead to macroscopic failure of the coating at later stages. Significantly longer exposures will thus be needed, which require a new design of the small electrochemical cell used in the SECM, for the effective duration of the experiments is currently limited by the natural evaporation of a very small volume of the electrolyte.

The results presented here concerning the time dependence of blisters growth, are of a preliminary nature, as they have been based on the observation of a single blister. A

rigorous kinetic description of blister formation will require monitoring a statistically-relevant number of individual features.

Acknowledgement:

We are grateful to the Ministerio de Educación y Ciencia (Madrid, Spain) within the framework of Project CTQ2005-06446/BQU, under which the present work was carried out. A Doctoral Grant to Y.G.-G. by the University of La Laguna and Cajacanarias (Tenerife, Spain) is gratefully acknowledged.

References:

1. J.E.O. Mayne, in *Corrosion*, vol. 2, L.L.Shreir, R.A. Jarman and G.T. Burstein (Eds.). Butterworths-Heinemann, Oxford, 1994, p. 14:22.
2. G. Grundmeier and A. Simões, in *Encyclopedia of Electrochemistry,* vol. 4, M. Stratmann and G.S. Frankel (Eds.). Wiley-VCH, Weinheim, 2003, p. 500.
3. M. Stratmann, R. Feser and A. Leng, *Electrochimica Acta*, **39** (1994) 1207.
4. M. Rohwerder and M. Stratmann, in *Analytical Methods in Corrosion Science and Engineering*, P. Marcus and F. Mansfeld (Eds). CRC Press, Boca Raton (FL), 2006, p.603.
5. F. Mansfeld, in *Analytical Methods in Corrosion Science and Engineering*, P. Marcus and F. Mansfeld (Eds). CRC Press, Boca Raton (FL), 2006, p.463.
6. K. Darowicki, P. Ślepski and M. Szociński, *Progress in Organic Coatings*, **52** (2005) 306.
7. W. Schmidt and M. Stratmann, *Corrosion Science*, **40** (1998) 1441.
8. A. Leng, H. Streckel and M. Stratmann, *Corrosion Science*, **41** (1999) 547, 599.
9. W. Fürbeth and M. Stratmann, *Corrosion Science*, **43** (2001) 207, 229, 243.
10. M. Rohwerder, E. Hornung and M. Stratmann, *Electrochimica Acta*, **48** (2003) 1235.
11. M. Doherty and J.M. Sykes, *Corrosion Science,* **46** (2004) 1265.
12. B. Reddy, M.J. Doherty and J.M. Sykes, *Electrochimica Acta*, **49** (2004) 2965.
13. J.M. Sykes and M. Doherty, *Corrosion Science*, **50** (2008) 2773.
14. M. Rohwerder, S. Isik-Uppenkamp and M. Stratmann, *Electrochimica Acta*, **54** (2009) 6058.
15. D.A. Worsley, S.M. Powell and H.N. McMurray, *Corrosion (NACE)*, **56** (2000) 492.

16. K. Ogle, V. Baudu, L. Garrigues and X. Philippe, *Journal of the Electrochemical Society*, **147** (2000) 3654.
17. J. Elvins, J.H. Sullivan, J.A. Spittle and D.A. Worsley, *Corrosion Engineering, Science and Technology,* **40** (2005) 43.
18. I.M. Zin, S.B. Lyon and A. Hussain, *Progress in Organic Coatings,* **52** (2005) 126.
19. A.M. Cabral, W. Trabelsi, R. Serra, M.F. Montemor, M.L. Zheludkevich and M.G.S. Ferreira, *Corrosion Science,* **48** (2006) 3740.
20. K. Ogle, S. Morel and D. Jacquet, *Journal of the Electrochemical Society*, **153** (2006) B1.
21. M.L. Zheludkevich, K.A. Yasakau, A.C. Bastos, O.V. Karavai and M.G.S. Ferreira, *Electrochemistry Communications*, **9** (2007) 2622.
22. S.V. Lamaka, M.L. Zheludkevich, K.A. Yasakau, R. Serra, S.K. Poznyak and M.G.S. Ferreira, *Progress in Organic Coatings,* **58** (2007) 127.
23. F. Thébault, B. Vuillemin, R. Oltra, K. Ogle and C. Allely, *Electrochimica Acta*, **53** (2008) 5226.
24. A.M. Simões, J. Torres, R. Picciochi and J.C.S. Fernandes, *Electrochimica Acta*, **54** (2009) 3857.
25. R.M. Souto, B. Normand, H. Takenouti and M. Keddam, *Electrochimica Acta*, (2009) ref. No. *EAST09-1133*.
26. J.-B. Jorcin, E. Aragon, C. Merlatti and N. Pébère, *Corrosion Science,* **48** (2006) 1779.
27. C.F. Zhong, X. Tang and Y.F. Cheng, *Electrochimica Acta*, **53** (2008) 4740.
28. C.F. Dong, A.Q. Fu, X.G. Li and Y.F. Cheng, *Electrochimica Acta*, **54** (2008) 628.
29. A.C. Bastos, A.M. Simões, S. González, Y. González-García and R.M. Souto, *Progress in Organic Coatings,* **53** (2005) 177.
30. Y. González-García, S. González and R.M. Souto, *Corrosion Science,* **47** (2005) 3312.
31. A. Simões, D. Battocchi, D. Tallman and G. Bierwagen, *Progress in Organic Coatings,* **63** (2008) 260.
32. Y. Shao, C. Jia, G. Meng, T. Zhang and F. Wang, *Corrosion Science,* **51** (2009) 371.
33. R.M. Souto, Y. González-García, S. González and G.T. Burstein, *Corrosion Science,* **46** (2004) 2621.
34. R.M. Souto, Y. González-García and S. González, *Corrosion Science,* **50** (2008) 1637.
35. R.M. Souto, Y. González-García and S. González, *Progress in Organic Coatings*, **65** (2009) 435.

36. A.J. Bard, F.-R. Fan and M.V. Mirkin, in *Electroanalytical Chemistry*, Vol. 18, A.J. Bard (Ed.). Marcel Dekker, New York, 1993, p. 243.
37. R.M. Souto, Y. González-García, S. González and G.T. Burstein, *Electroanalysis*, (2009) in press.
38. C. Bragato, S. Daniele, M.A. Baldo and G. Denuault, *Annali di Chimica*, **92** (2002) 153.
39. R.M. Souto, L. Fernández-Mérida and S. González, *Electroanalysis*, (2009) in press.
40. Y. González-García, S. González and R.M. Souto, *Corrosion Science,* **49** (2007) 3514.

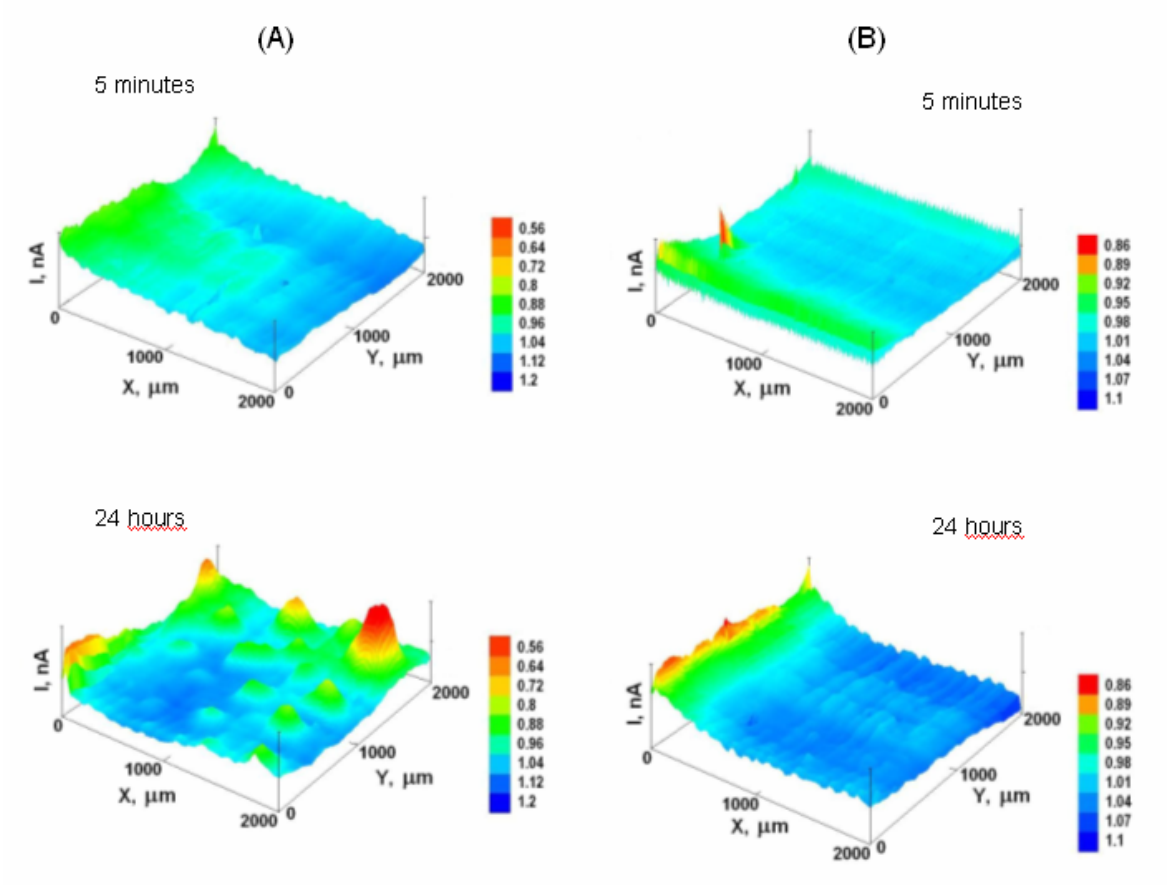

Figure 1 - SECM measurement on a polyurethane-coated carbon steel plate. Tip-substrate distance: 15 µm. Scan rate: 30 µm s^{-1}. Tip potential: +0.50 V *vs*. Ag/AgCl/KCl (saturated) reference electrode. Values of *Z* axis: Current, nA. The figures represent an area of 2000 µm x 2000 µm in *X* and *Y* directions. From top to bottom: 5 minutes, 24 hours immersion in the test solution: (A) 0.1 M KCl + 0.5 mM ferrocene-methanol, and (B) 0.1 M K_2SO_4 + 0.5 mM ferrocene-methanol.

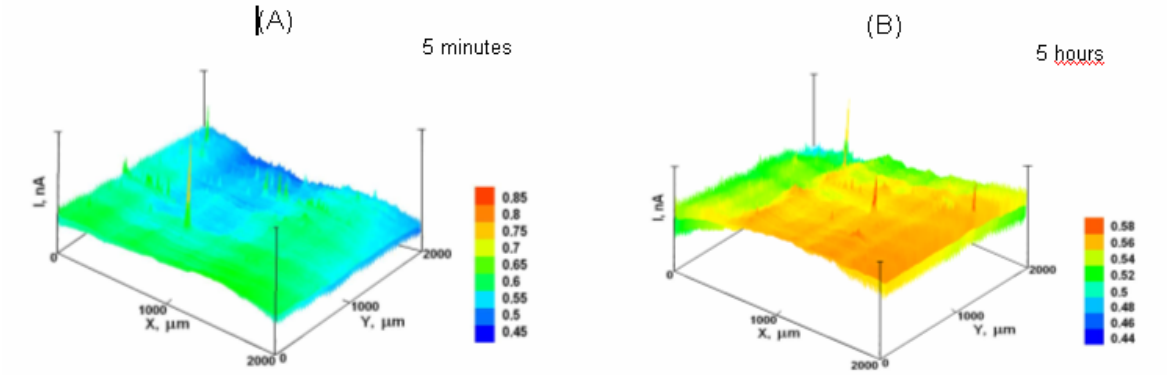

Figure 2 - SECM measurement on a defective polyurethane-coated carbon steel plate immersed in 0.1 M KCl + 0.5 mM ferrocene-methanol solution. Tip-substrate distance: 15 µm. Scan rate: 60 µm s^{-1}. Tip potential: +0.50 V *vs*. Ag/AgCl/KCl (saturated) reference electrode. Values of *Z* axis: Current, nA. The figures represent an area of 2000 µm x 2000 µm in *X* and *Y* directions. The images were taken after: (A) 5 minutes, and (B) 5 hours immersion in solution.

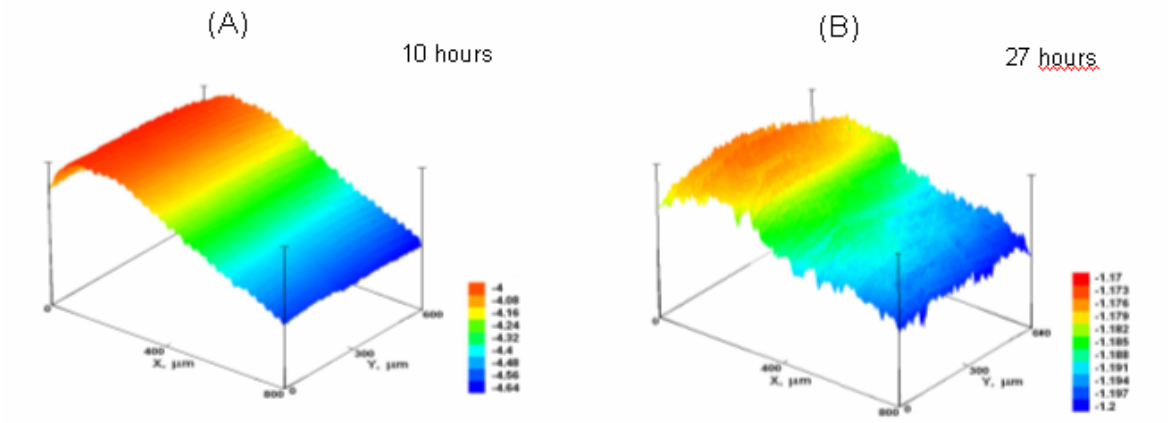

Figure 3 - SECM measurement on a polyurethane-coated carbon steel plate immersed in 0.1 M KCl solution. Tip-substrate distance: 15 µm. Scan rate: 30 µm s^{-1}. Tip potential: -0.60 V *vs*. Ag/AgCl/KCl (saturated) reference electrode. Values of *Z* axis: Current, nA. The figures represent an area of 800 µm x 600 µm in *X* and *Y* directions. The images were taken after: (A) 10, and (B) 27 hours immersion in solution.

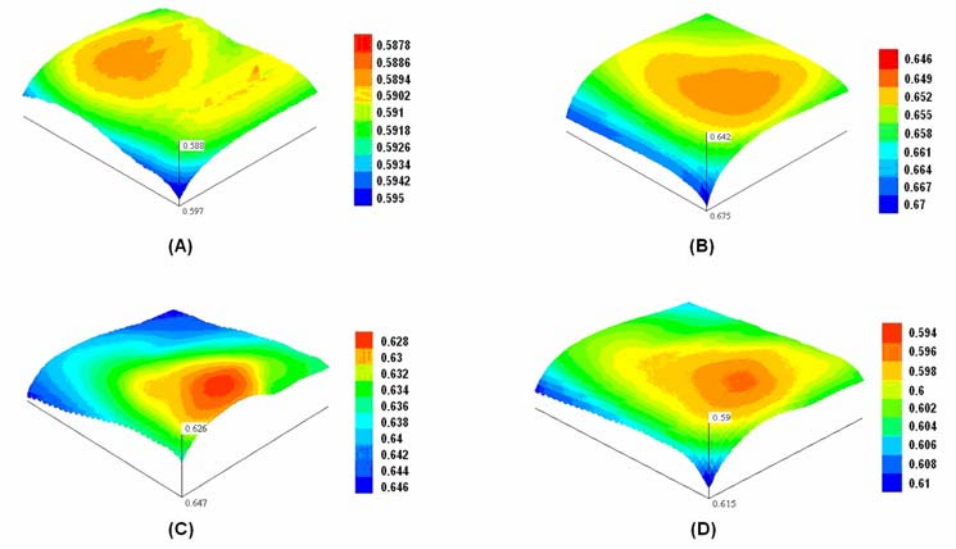

Figure 4 - SECM measurement on a polyurethane-coated carbon steel plate immersed in 0.1 M KCl + 0.5 mM ferrocene-methanol solution. Tip-substrate distance: 15 µm. Scan rate: 30 µm s^{-1}. Tip potential: +0.50 V *vs*. Ag/AgCl/KCl (saturated) reference electrode. Values of *Z* axis: Current, nA. The figures represent an area of 200 µm x 200 µm in *X* and *Y* directions. The images were taken after: (A) 40 min, (B) 70 min (C) 140 min, and (D) 22 hours immersion in solution.

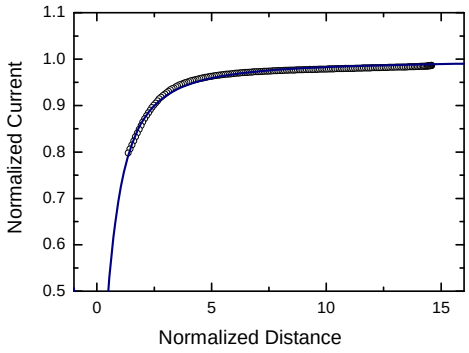

Figure 5 - Approach curve measured at the SECM-tip in 0.1 M KCl + 0.5 mM ferrocene-methanol solution shortly after the polyurethane-coated carbon steel sample was exposed to the solution. $I = i / i_{lim}$ is the dimensionless tip current, and $L = d / a$ is the dimensionless distance between the sample and the tip. (○) Experimental curve, and (——) fitting with RG = 2.03. Tip potential: +0.50 V *vs*. Ag/AgCl/KCl (saturated) reference electrode. The movement of the microelectrode was stopped when the current measured at the tip decreased to an 80% of the steady-state value in the bulk of the electrolyte.

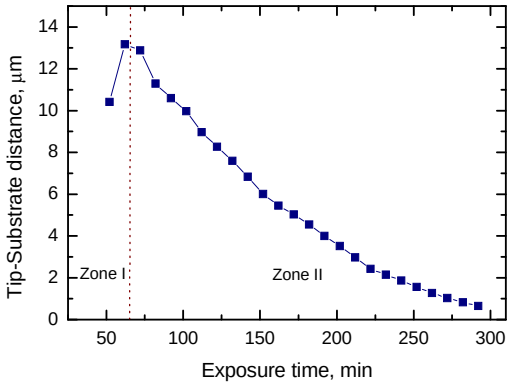

Figure 6 - Distance between the tip and the summit of a blister developed on a polyurethane-coated CCS specimen immersed in 0.1 M KCl + 0.5 mM ferrocene-methanol as a function of exposure time. The bulge under consideration is the same depicted in Figure 4.